

Supporting Information

Worm-like amorphous MnO₂ nanowires grown on textiles for high-performance flexible supercapacitors

Peihua Yang,^{‡ a} Yuzhi Li,^{‡a} Ziyin Lin,^b Yong Ding,^b Song Yue,^a Ching Ping Wong,^b Xiang Cai,^c Shaozao Tan,^c Wenjie Mai^{*ab}

^a Department of Physics and Siyuan Laboratory, Jinan University, Guangzhou, Guangdong 510632, China

^b School of Materials Science and Engineering, Georgia Institute of Technology, Atlanta, Georgia 30332, United States

^c Department of Chemistry, Jinan University, Guangzhou, Guangdong 510632, China

^{*}Address correspondence to wenjiemai@gmail.com (W.J.Mai)

[‡]P.H.Yang and Y.Z.Li contributed equally to this work.

Experimental section

Synthesis of MnO₂ nanowires

WO₃-assisted worm-like MnO₂ (WL-MnO₂) NWs were grown on carbon fabric by anodic electrodeposition technique in a three-electrode cell.¹ A graphite rod and Ag/AgCl electrode were used as the counter electrode and reference electrode, respectively. Before the deposition process, the carbon fabric was treated by ethanol. In a typical process, a 15 mL suspension containing 0.01 M manganese acetate and 15 mg WO₃ nanoparticles (50 nm) was sonicated for 20 min. Then the electrodeposition was conducted at a constant current of 0.5 mA/cm² at 70 °C. The carbon fabric was taken out from the reaction vessel and washed with a deionized water thoroughly after the deposition process continued for a certain time. After the deposition process, we found that the suspension still kept turbid. For comparison, cotton-like structure MnO₂ (CL-MnO₂) was directly grown on carbon cloth without WO₃ nanoparticle *via* a same procedure. The mass loading of WL-MnO₂ and CL-MnO₂ in 15 min deposition was about 0.248 mg/cm² and 0.251mg/cm² determined by inductively coupled plasma atomic emission spectroscopy (ICP-AES), respectively.

Fabrication of the solid-state SC

The SC device was assembled by using two pieces of WL-MnO₂ NWs (15 min deposition time) electrodes with a separator (NKK TF40, 40 µm) and PVA/LiCl gel as a solid electrolyte. PVA/LiCl gel was prepared by mixing LiCl (12.6 g) and PVA (6 g) in 60 mL deionized water and heated at 85 °C with stirring for 2 h. The electrodes and separator were immersed in the gel electrolyte about 5 min, and then assembled together. The device was kept at 60 °C for 6 h to remove excess water in the electrolyte. After the gel electrolyte became solid, the thickness of the device was around 0.8 mm and the effective contact area of the electrodes was about 1 cm².

Characterization

The structural properties of electrode materials were characterized by field-emission scanning electron microscopy (SEM, ZEISS ULTRA 55), transmission electron microscopy (TEM, FEI TECNAI F30) equipped with an energy dispersive X-ray spectrometer (EDS), X-ray diffraction (XRD, X'Pert PRO Alpha-1), and X-ray Photoelectron Spectroscopic (XPS, Thermo K-alpha). The electrochemical properties of the products were investigated employing a VersaSTAT 3 (Princeton Applied Research) electrochemical workstation. The cycle life was measured through a battery test system (Neware BTS). The amount of Mn and W was determined by inductively coupled plasma atomic emission spectroscopy (ICP-AES, OPTIMA 2000DV). For a single electrode test, a piece of electrode (effective area *ca.* 1 cm²) was dipped into a 0.5 M Na₂SO₄ solution at room temperature. Ag/AgCl reference electrode and graphite rod counter electrode were used in the measurement.

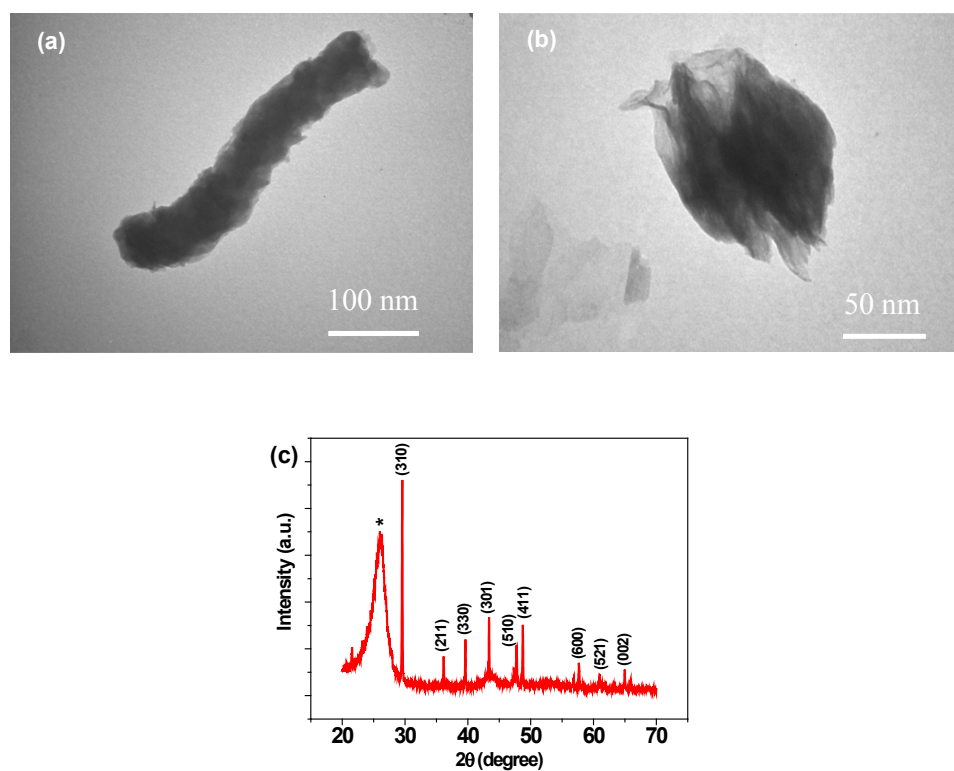


Figure S1 TEM images of (a) WL-MnO₂ and (b) CL-MnO₂. (c) XRD pattern of CL-MnO₂. All the diffraction peaks can be exclusively indexed as the tetragonal α -MnO₂ (JCPDS 44-0141)² except the crystalline peak at 26.2° coming from carbon fabric substrate.

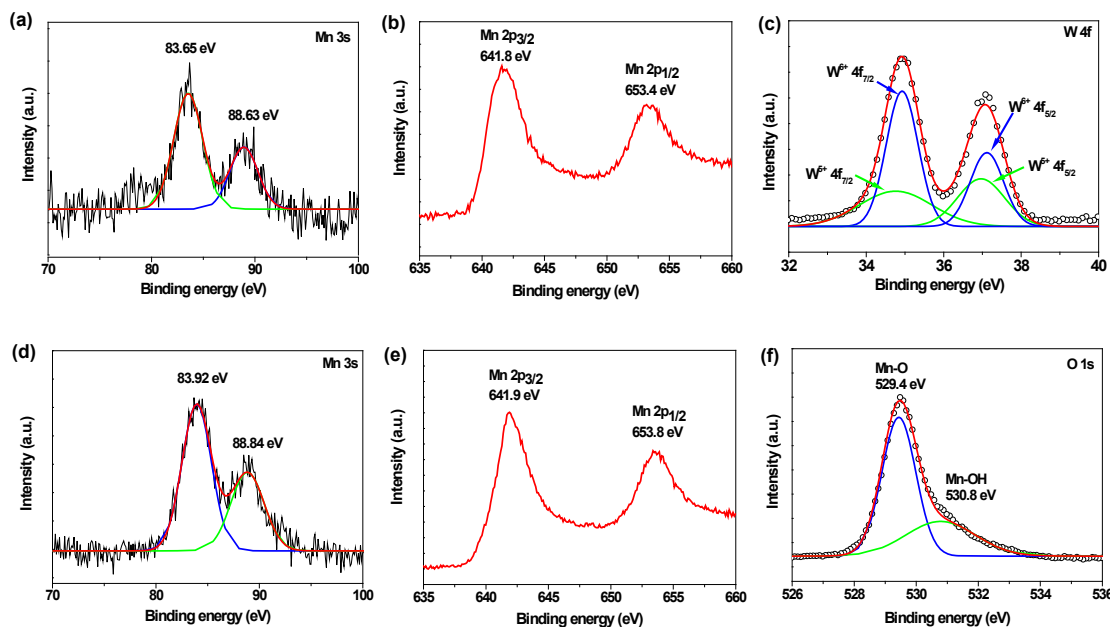


Figure S2 Core level (a) Mn 3s, (b) Mn 2p, and (c) W 4f XPS spectra collected for the WL-MnO₂ NWs. As reported previously,³⁻⁴ the Mn oxidation state can be determined from the binding energy width (ΔE) between the separated Mn 3s peaks caused by multiplet splitting. By reference to the ΔE data of 5.79, 5.50, 5.41 and 4.78 eV acquired from genuine samples of MnO, Mn₃O₄, Mn₂O₃ and MnO₂, respectively, the possible valence of Mn in the WL-MnO₂ NWs ($\Delta E=4.98$ eV) is +3.68. Mn 2p_{3/2} and Mn 2p_{1/2} peaks were located at 641.8 and 653.4 eV. The W 4f spectrum can be decomposed into four peaks. The strong peaks located at 34.93 and 37.12 eV are corresponding to W⁶⁺ oxidation state, while the weak peaks located at 34.76 and 36.96 eV are corresponding to W⁵⁺ oxidation state.⁵⁻⁷ According to the intensity of the peaks, the valence of tungsten should be closer to +6. (d) Mn 3s, (e) Mn 2p, and (f) O 1s XPS spectra collected for the CL-MnO₂. The possible valence of Mn in the CL-MnO₂ NWs ($\Delta E=4.92$ eV) is +3.78. Mn 2p_{3/2} and Mn 2p_{1/2} peaks were located at 641.9 and 653.8 eV. The band at 529.4 and 530.8 eV can be assigned to the oxygen bond of Mn-O and Mn-OH, respectively.

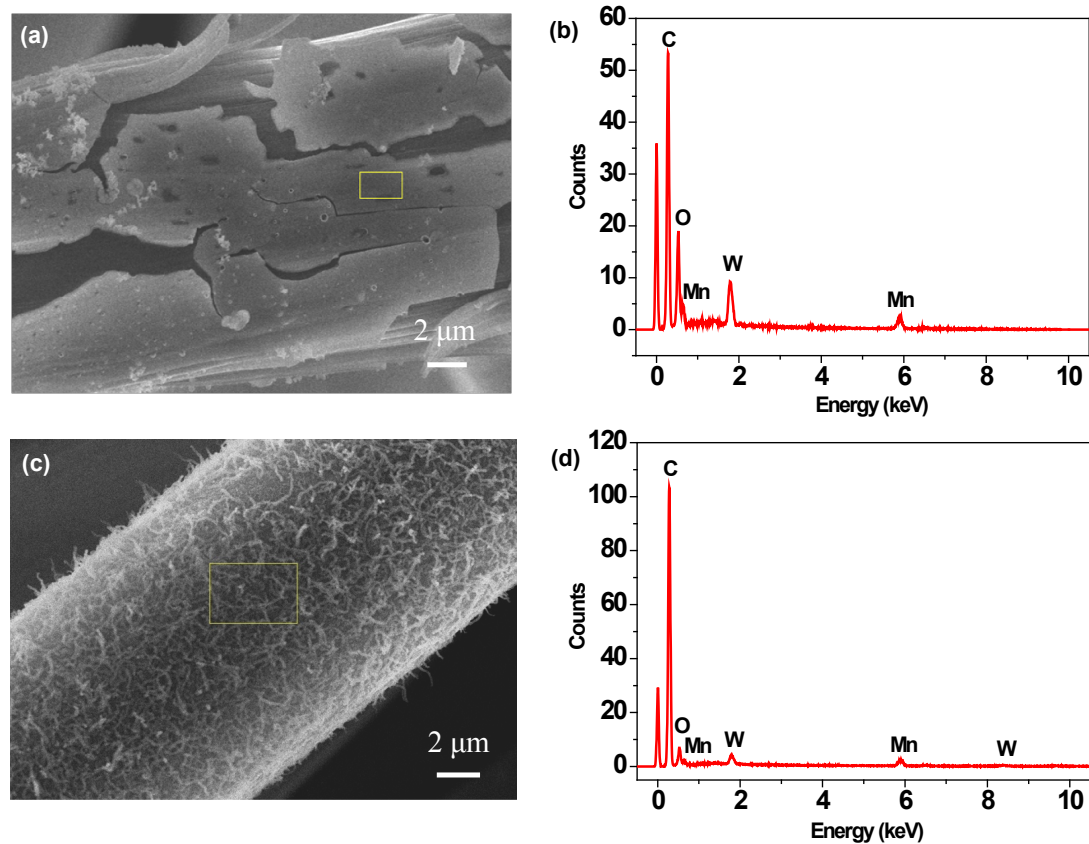


Figure S3 (a) SEM image and (b) EDS spectrum of WL- MnO_2 obtained in 5 min deposition, (c) SEM image and (d) EDS spectrum of WL- MnO_2 obtained in 15min deposition.

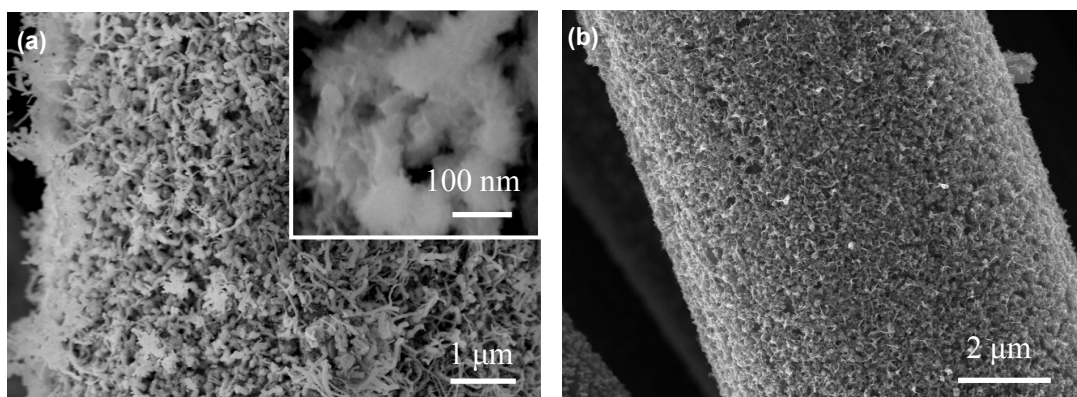


Figure S4 SEM images of (a) WL-MnO₂ in 30 min deposition and (b) CL-MnO₂ in 5 min deposition.

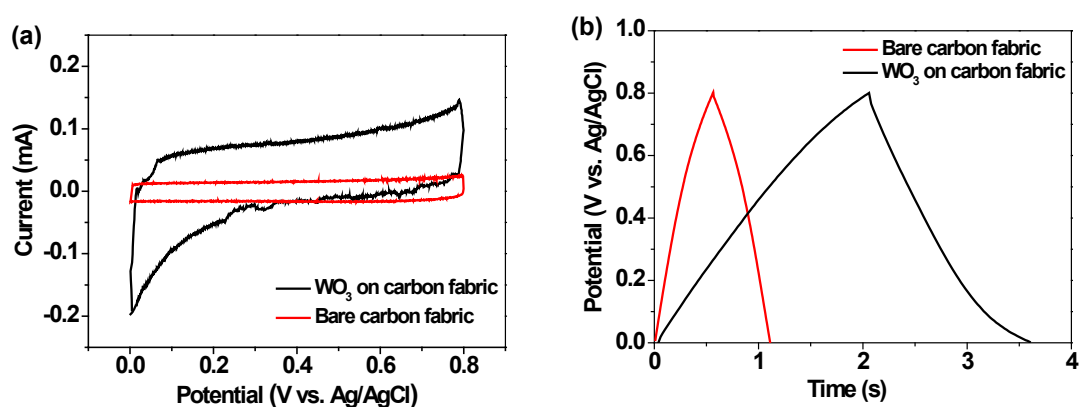


Figure S5 (a) CV curves collected at a scan rate of 100 mV/s and (b) galvanostatic charge/discharge curves at 0.25 mA for bare carbon fabric and WO₃ deposited on carbon fabric with 0.5 M Na₂SO₄ and 1.0 mg/mL WO₃ in 15 min deposition.

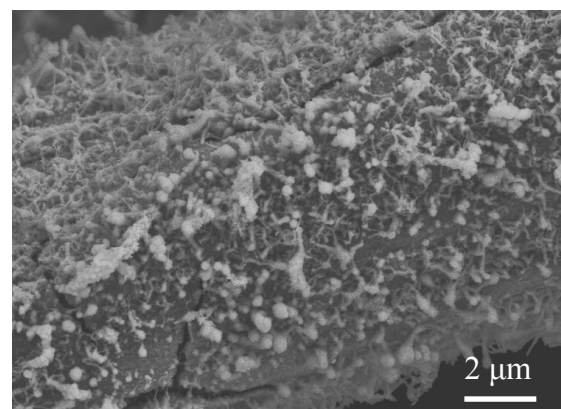


Figure S6 SEM image of WL-MnO₂ after 1000 cycles in 0.5 M Na₂SO₄ at a scan rate of 100 mV/s.

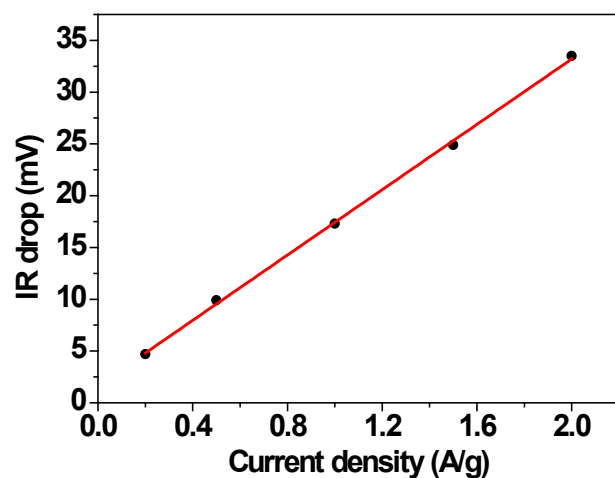


Figure S7 IR drops of solid-state SC vs current density. R_s can be calculated from the fitting, which is about 15.8Ω .

Calculations

1. Single electrode:

Since the capacitance of WO_3 and carbon fabric are extremely small compared to MnO_2 (Figure S5), so all the calculations is based on MnO_2 material. The specific capacitance (C_s , F/g) of the single electrode could be calculated from their charge/discharge curves by the following equations

$$C_s = \frac{I\Delta t}{m\Delta U}$$

where I is the discharge current, Δt is the discharge time, ΔU is the potential window during the discharge process removed the IR drop, and m is the active material mass of the electrode.

2. SC device:

The volumetric capacitance (C_v , F/cm³) and specific capacitance (C_s , F/g) of the SC device were calculated from their charge/discharge curves according to the following equations

$$C_v = \frac{I\Delta t}{V\Delta U} \quad C_s = \frac{4I\Delta t}{M\Delta U}$$

where I is the discharge current, Δt is the discharge time, ΔU is the potential window during the discharge process removed the IR drop, M is the total mass of active materials in an SC device, and V is the cell volume (about 0.08 cm³).

The coulombic efficiency of the SC were characterized by charge/discharge process according to

$$\eta = \frac{\Delta t_d}{\Delta t_c}$$

where Δt_d and Δt_c represent the discharge and charge time, respectively.

Energy density (E , Wh/kg) and maximum power density (P , kW/kg) could be calculated as

$$E = \frac{C_s U^2}{8}$$

$$P = \frac{U^2}{4R_s M}$$

$$R_s = \frac{U_{IR}}{2I}$$

where C_s is specific capacitance calculated before, U is the cell voltage, U_{IR} is the IR drop and M is the total mass of active materials in an SC device. R_s can be got from the fitting of IR drop vs current density, is about 15.8 Ω.

References

1. D. Liu, Q. Wang, L. Qiao, F. Li, D. Wang, Z. Yang and D. He, *Journal of Materials Chemistry*, 2012, **22**, 483-487.
2. L. Gong, X. Liu and L. Lu, *Materials Letters*, 2012, **67**, 226-228.
3. M. Chigane and M. Ishikawa, *Journal of The Electrochemical Society*, 2000, **147**, 2246-2251.
4. Y. Cheng, S. Lu, H. Zhang, C. V. Varanasi and J. Liu, *Nano Letters*, 2012, **12**, 4206-4211.
5. X. Lu, T. Zhai, X. Zhang, Y. Shen, L. Yuan, B. Hu, L. Gong, J. Chen, Y. Gao, J. Zhou, Y. Tong and Z. L. Wang, *Advanced Materials*, 2012, **24**, 938-944.
6. X. Zhang, L. Gong, K. Liu, Y. Cao, X. Xiao, W. Sun, X. Hu, Y. Gao, J. Chen, J. Zhou and Z. L. Wang, *Advanced Materials*, 2010, **22**, 5292-5296.
7. B. Cao, J. Chen, X. Tang and W. Zhou, *Journal of Materials Chemistry*, 2009, **19**, 2323-2327.